Original Contribution

Vascular Tissue-Type Plasminogen Activator Promotes Intracranial Aneurysm Formation

Paul-Emile Labeyrie, MD, MSc*; Romain Goulay, PhD*; Sara Martinez de Lizarrondo, PhD; Marie Hébert, PhD; Maxime Gauberti, PhD; Eric Maubert, PhD; Barbara Delaunay, MSc; Benjamin Gory, MD, PhD; Francesco Signorelli, MD, MSc; Francis Turjman, MD, PhD; Emmanuel Touzé, MD, PhD; Patrick Courthéoux, MD†; Denis Vivien, PhD*; Cyrille Orset, PhD*

Background and Purpose—Although the mechanisms that contribute to intracranial aneurysm (IA) formation and rupture are not totally elucidated, inflammation and matrix remodeling are incriminated. Because tPA (tissue-type plasminogen activator) controls both inflammatory and matrix remodeling processes, we hypothesized that tPA could be involved in the pathophysiology of IA.

Methods—Immunofluorescence analyses of tPA and its main substrate within the aneurysmal wall of murine and human samples were performed. We then compared the formation and rupture of IAs in wild-type, tPA-deficient and type 1 plasminogen activator inhibitor–deficient mice subjected to a model of elastase-induced IA. The specific contribution of vascular versus global tPA was investigated by performing hepatic hydrodynamic transfection of a cDNA encoding for tPA in tPA-deficient mice. The formation and rupture of IAs were monitored by magnetic resonance imaging tracking for 28 days.

Results—Immunofluorescence revealed increased expression of tPA within the aneurysmal wall. The number of aneurysms and their symptomatic ruptures were significantly lower in tPA-deficient than in wild-type mice. Conversely, they were higher in plasminogen activator inhibitor–deficient mice. The wild-type phenotype could be restored in tPA-deficient mice by selectively increasing circulating levels of tPA via hepatic hydrodynamic transfection of a cDNA encoding for tPA.

Conclusions—Altogether, this preclinical study demonstrates that the tPA present in the blood stream is a key player of the formation of IAs. Thus, tPA should be considered as a possible new target for the prevention of IAs formation and rupture. **(*Stroke*. 2017;48:00-00. DOI: 10.1161/STROKEAHA.117.017305.)**

Key Words: animals ■ intracranial aneurysm ■ mice ■ physiopathology ■ tissue plasminogen activator

Intracranial aneurysms (IAs) are brain vascular malformations, with a prevalence of 3% to 5% in the general population.[1–3] In most cases, IA causes no symptom and goes unnoticed. However, the rupture of an IA causes a subarachnoid hemorrhage leading to high mortality and disability rates.[3] Despite recent therapeutic advances, no reliable noninvasive treatment has proved efficient to prevent aneurysm growth and rupture.[4–6] Thus, a better understanding of the pathophysiology of IAs is mandatory to develop new preventive and therapeutic strategies.[2,6]

Aneurysms originate from a series of events starting with the activation of endothelial cells leading to inflammatory processes and ultimately to a progressive loss of integrity of the arterial wall.[7–9] Some of the actors involved in this cascade of events have been identified, including macrophages, lymphocytes, and their effector molecules (like chemokines and inflammatory cytokines)[7,10,11] and matrix metalloproteinases (MMPs).[12]

tPA (tissue-type plasminogen activator) is a serine protease expressed and released by endothelial cells, where it displays its fibrinolytic role through activation of plasminogen into plasmin.[13,14] Interestingly, an increased expression of tPA has been observed in aortic aneurysms.[15–18] Furthermore, the tPA–plasmin axis is well known to promote inflammatory

Received March 20, 2017; final revision received June 8, 2017; accepted July 5, 2017.

From the Department of Physiopathology and Imaging of Neurological Disorders, INSERM U1237, UNICAEN, GIP Cyceron, France (P.-E.L., R.G., S.M.d.L., M.H., M.G., E.M., B.D., E.T., P.C., D.V., C.O.); Department of Interventional Neuroradiology (P.-E.L., B.G., F.T.) and Department of Neurosurgery (F.S.), Hôpital Wertheimer, University Lyon 1, Bron, France; and Department of Neurology (E.T.), Department of Neuroradiology (P.C.), and Department of Clinical Research (D.V.), CHU Caen, University Caen Normandie, France.

Guest Editor for this article was Christoph Kleinschnitz, MD.

*Drs Labeyrie, Goulay, Vivien, and Orset contributed equally.

†Contributing author Patrick Courthéoux passed away in April 2016.

The online-only Data Supplement is available with this article at http://stroke.ahajournals.org/lookup/suppl/doi:10.1161/STROKEAHA.117.017305/-/DC1.

Correspondence to Denis Vivien, PhD, Department of Physiopatholgy and Imaging of Neurological Disorders, INSERM U1237, University Caen Normandie, GIP Cyceron, Bd Becquerel, BP5229, 14074 Caen, France. E-mail vivien@cyceron.fr

processes[19,20] and to enhance extracellular matrix degradation both known to contribute to IAs generation.[15,19,20] Because IAs are strongly associated with inflammatory processes and remodeling of the extracellular matrix,[11,12] we hypothesized that tPA could contribute to the formation or rupture of IAs.

Methods

An expanded materials and methods section is available as an online-only Data Supplement.

Experiments were performed in accordance with European union directives (2010/63/UE) and French ethical laws (act no. R214; 87–137; Ministère de l'Agriculture) guidelines and approved by the local and regional ethics committees (authorization code, CENOMEXA 0113-03). All experiments were performed following the ARRIVE guidelines (Animal Research: Reporting of In Vivo Experiments; http://www.nc3rs.org.uk).

Induction of IAs

IAs were induced as described by Hashimoto et al[11,21] in 3 different mouse strains: tPA−/− (n=31), plasminogen activator inhibitor-1 (PAI-1) knockout mice (n=12), and their wild-type (WT) littermates (n=12) all on a C57BL/6J background.

Briefly, stereotaxic injection in the right basal cistern of 2.5 µL of elastase was realized in deeply anesthetized animals. Followed by subcutaneous implantation of an osmotic pump (p1001; Alzet) filled with angiotensin II (Sigma Aldrich). The profile of systemic hypertension induced by angiotensin II was assessed by repeated blood pressure measurements using the tail-cuff method. At day 2, a magnetic resonance imaging (MRI) was performed to exclude animals presenting a brain hemorrhage caused by the stereotaxic injection. Each animal was evaluated for inclusion criterion using a semiquantitative aneurysm induction invasiveness score (Figure IA in the online-only Data Supplement). All animals with a score >7 were excluded from the study. Animals were analyzed twice a day for detection of neurological symptoms and weight loss during a period of 28 days postinduction. Symptomatic mice were immediately scanned by MRI for the identification of intracranial hemorrhages and ruptured aneurysms. The period before symptoms occurs, mice were considered as symptom-free surviving animals, and this time was evaluated and quoted per day after aneurysm induction. At 28 days marking the term of the study, all asymptomatic mice were scanned by MRI before euthanasia because their MRI analyses were also used to estimate the number of unruptured aneurysms and the absence of bleeding. IA lesions were observed on each mouse, at the acute phase of rupture when symptomatic and at the end of the experiment (day 28) in the absence of rupture.

MRI Analysis

Experiments were performed on a Pharmascan 7T/12 cm system using surface coils (Bruker) in anesthetized mice. T2*-weighted sequence was used to detect intracranial hemorrhage as a specific hyposignal.[22] 3-dimensional T1 contrast enhanced weighted sequence after intraperitoneal gadolinum injection (Gadovist 1 mg/kg; Guerbet) was performed to visualize IA defined as an abnormal sacciform outpouching of the wall of intracranial arteries of which the diameter is >150% of the parent artery diameter.[21]

Hydrodynamic Transfection of tPA

Generation of pLIVEPlasmids

The coding sequence for rat tPA was inserted into a mouse hepatocyte specific plasmid (pLIVE; Figure IB in the online-only Data Supplement).

Hydrodynamic Transfection

Hydrodynamic transfections were performed as described previously.[23,24] To assess the time course of gene delivery, we have previously investigated[24] the presence of active and free (noncomplexed) plasmatic tPA by direct fibrin zymography following SDS-PAGE (Sodium Dodecyl Sulfate Polyacrylamide Gel Electrophoresis), performed from plasma samples harvested before and after hepatic (hydrodynamic) transfection at days 1, 2, 3, 5, 7, and 14.[24] Then, PA−/− mice considered for IA induction were injected 2 days before induction with 100 µg of pLIVE vector encoding for tPA (n=11) or empty pLIVE vector (n=9; Figure IB and IC in the online-only Data Supplement). Then, sentinel mice induced for IAs were used to control levels of active plasmatic tPA, 24 hours after hydrodynamic transfection (Figure ID in the online-only Data Supplement; time when the highest plasmatic levels) as described previously.[24] Human tPA (Actilyse; Boehringer Ingelheim) and plasmin (Enzyme Research Laboratories) were used as loading controls.

Immunohistochemistry

Mouse Tissue Samples

Each mouse was anesthetized and transcardially perfused with cold heparinized saline followed by 100 mL of fixative solution. Brains were cryoprotected before freezing in Tissue-Tek (Miles Scientific).

Human Sample

Human aneurysm samples were obtained during microsurgery by resecting the aneurysm sac distal to the clip closing the neck (F.S.). Samples were obtained from a 42-year-old woman, who experienced subarachnoid hemorrhage after a rupture of a 7-mm large, middle cerebral artery IA. Tissues were immediately stored for 2 hours in fixative then cryoprotected before freezing in Tissue-Tek.

For both human and mouse tissue samples, cryomicrotome-cut transversal sections (12 µm) were collected on polylysine slides and stored at −80°C before processing. Mouse and human tissue sections were incubated overnight with primary antibodies as described in the corresponding legend and detailed in the Methods in the online-only Data Supplement. For each animal, vascular wall and aneurysm were analyzed.

Statistical Analysis

All results were expressed in the form of mean. Continuous variables were described as median and interquartile range and compared using the nonparametric Kruskal–Wallis test. Categorical variables were compared using χ^2 or Fisher exact test (unilateral test), as appropriate (SPSS 19, SPSS). The survival analyses were performed by using Kaplan–Meier and log-rank tests. The mice that did not show aneurysm formation were not excluded from the analysis. A P value ≤0.05 was considered as significant.

Results

tPA and Plasmin Are Present in the Arterial Wall of Aneurysmal Cerebral Arteries

IAs were induced and monitored as described (Figure 1A) in WT mice (n=12). This induction allowed forming sacciform aneurysms that can spontaneously rupture. Detection of symptomatic aneurysmal ruptures was addressed daily via a neurological score.[21,25] Symptomatic animals were immediately analyzed by MRI to assess the presence of intracranial bleedings and ruptured aneurysms (Figure 1B). Ruptures of IAs were confirmed by macroscopic visualization of harvested brains (Figure 1B). MRI for IAs detection perfectly matched with macroscopic observations (Figure 1C). The presence of tPA and plasminogen/plasmin were investigated in aneurysmal arteries and compared with normal contralateral arteries by immunohistochemistry. IA walls showed luminal bloating and asymmetrical wall thickening at multiple vascular localizations, especially around the distal intracerebral bifurcations

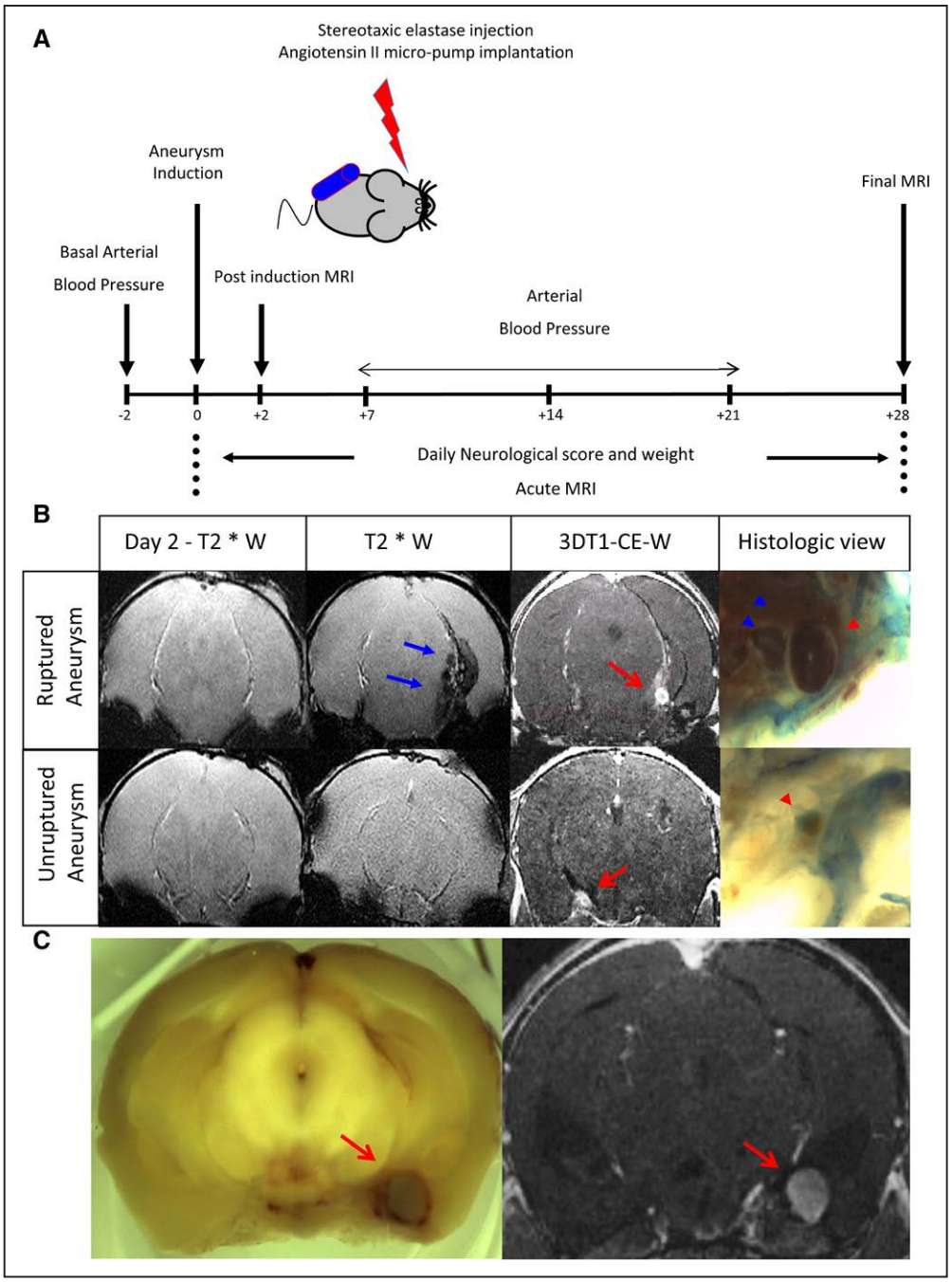

Figure 1. Experimental protocol. **A**, Six-weeks-old male mice maintained hypertensive by a chronic infusion of angiotensin II received a single stereotaxic injection of elastase to induce IAs. A clinical score and an magnetic resonance imaging (MRI) follow-up during the next 28 days allowed us to identify symptomatic and asymptomatic IA. **B**, At day 2, a T2*W (T2*-weighted) sequence was performed to exclude bleeding caused by the stereotaxic injection itself. **Top**, at day 7, symptomatic mice were subjected to MRI analyses: the T2*W sequence showed the appearance of a hyposignal (blue arrow) on the subarachnoid spaces; the 3-dimensional T1 contrast enhanced weighted (3DT1-CE-W) confirmed the presence of an IA (red arrow). The macroscopic analysis confirmed a bleeding (blue arrow head) and the presence of a ruptured aneurysm (red arrow head). **Bottom**, a MRI was performed on asymptomatic mice at day 28 showing the absence of bleeding on T2*W but the presence of an unruptured aneurysm (red arrow) confirmed by macroscopic examination (red arrow head). **C**, Higher magnification of the correlation between MRI (**left**) and the histological (**right**) identification of aneurysms.

when compared with contralateral arteries (Figure 2A). A massive tPA-positive immunostaining was revealed in the peripheral parts of the media and the adventitia for both ruptured and unruptured IAs (Figure 2B), with only a slight tPA-positive staining in the luminal part of the intima of normal arteries (Figure 2C).Immunostainings also revealed the presence of plasminogen/plasmin in the arterial walls of both ruptured and unruptured IA with a same distribution in the media of the pathological arterial walls (Figure 2B). Interestingly, immunostainings performed from human tissue samples also revealed the presence of tPA and plasminogen/plasmin within the arterial wall of IA arteries (Figure 2D).

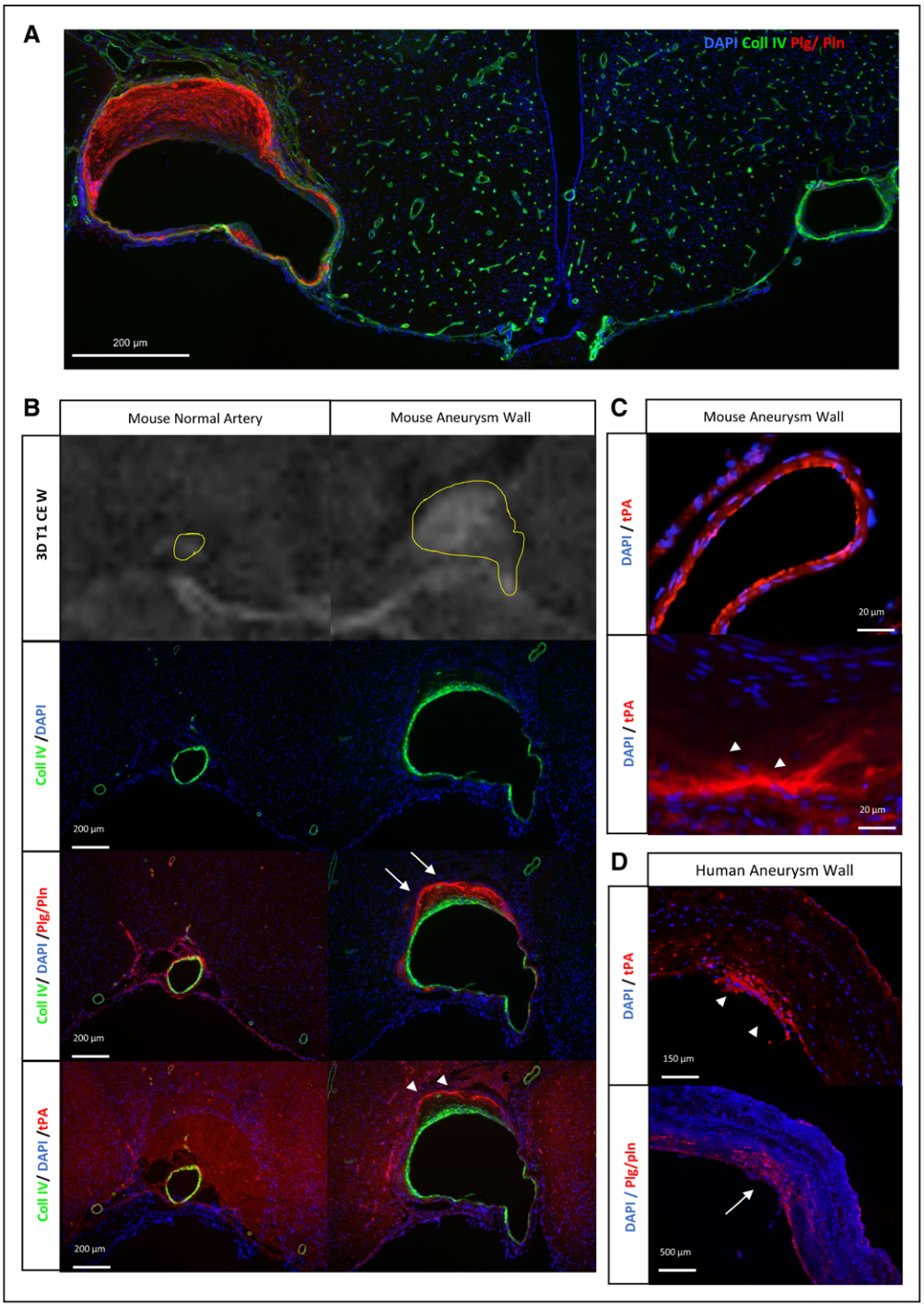

Figure 2. Overexpression of tPA (tissue-type plasminogen activator) and of plasminogen/plasmin within the aneurysmal wall. **A**, Representative immunohistochemistries performed from wild-type (WT) mice (n=10) displaying unruptured intracranial aneurysms (collagen-IV [Coll IV] in green, plasminogen [Plg]/plasmin [Pln] in red, and 4′,6-diamidino-2-phenylindole in blue). An aneurysm can be visualized on the **left** and a healthy contralateral artery on the **right**. **B**, Representative immunohistochemistries performed from WT mice displaying unruptured intracranial aneurysms for both Pln/Plg (white arrow) and tPA (white arrow head). An aneurysmal artery can be visualized on the **right** and a healthy contralateral artery on the **left**. **C**, Immunohistochemistries with high magnification on WT mice showing the endothelial repartition of tPA in normal artery (**top**) as its parietal presence in the aneurysm (white arrow head, **bottom**). **D**, Representative immunohistochemistries performed from intracranial aneurysms harvested on human after microsurgical clipping, showing the presence of tPA (white arrow head) and Plg/Pln (white arrow). Scale bars: **A**, 200 µm; **B**, 200 µm; **C**, 20 µm; and **D**, 150 µm, 500 µm.

Deletion of tPA Protects Against IAs Formation and Rupture

The influence of endogenous tPA on the formation and rupture of IAs was investigated in tPA-deficient (tPA–/–; n=12), PAI-1–deficient (PAI–/–; n=12), and compared with WT littermates (n=12). No significant difference in the mean systolic blood pressure was observed between groups (Figure IIA in the online-only Data Supplement). Similarly, aneurysm

induction invasiveness scores were not significantly different between groups (Figure IIB in the online-only Data Supplement). Patterns of aneurysms (no aneurysm, unruptured aneurysms, and ruptured aneurysms) between groups are shown in Figure 3A. tPA–/– animals were resistant to aneurysms formation (P=0.004) and subsequent ruptures (P=0.017) when compared with WT animals. Indeed, whereas only 40% of tPA–/– mice (n=10) presented at least 1 aneurysm

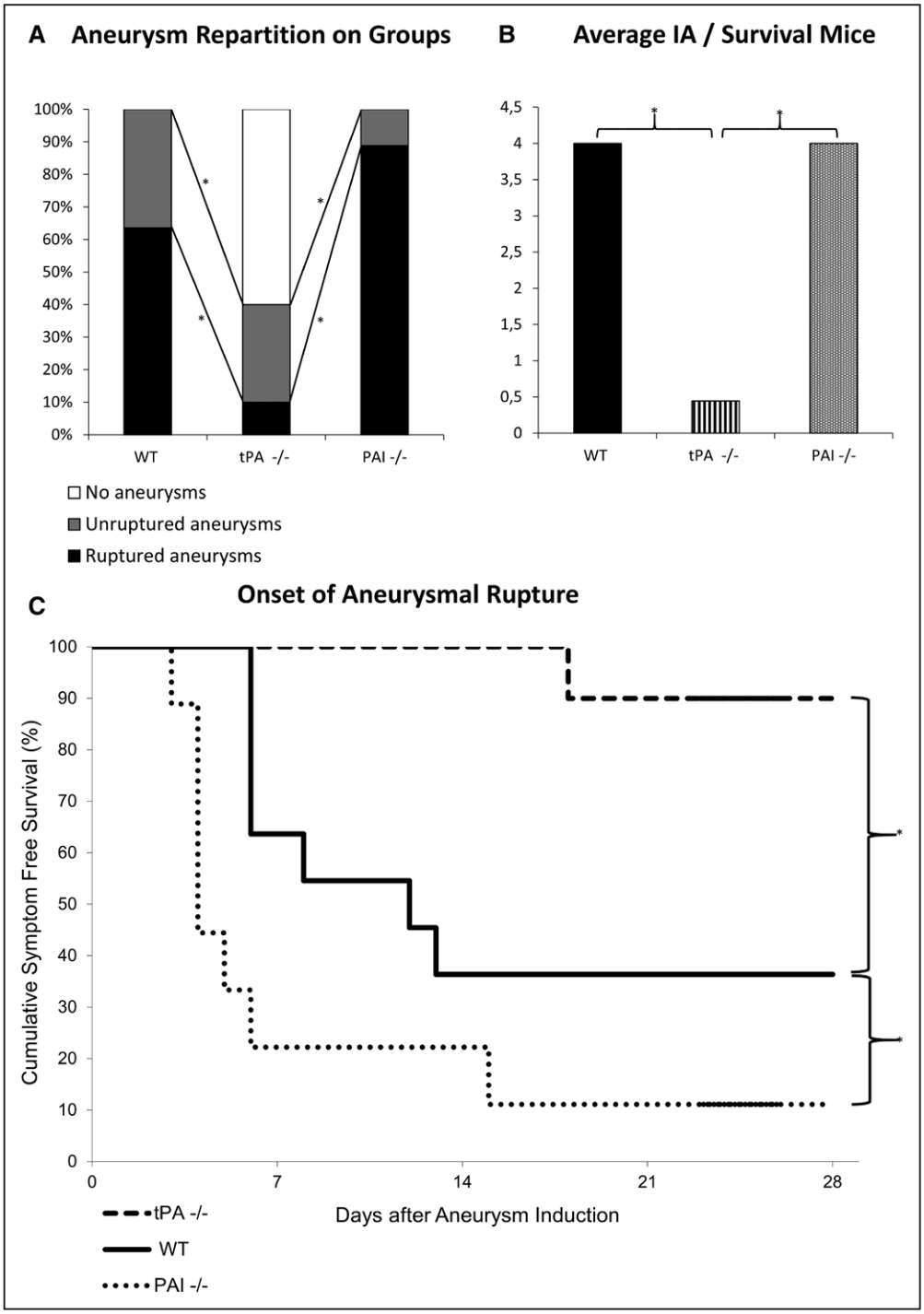

Figure 3. Lack of tPA (tissue-type plasminogen activator) protects against intracranial aneurysms formation and rupture. Intracranial aneurysms (IAs) were induced in tPA-deficient (tPA–/–), plasminogen activator inhibitor-1 (PAI-1)–deficient (PAI–/–), and wild-type (WT) mice. **A**, Aneurysm repartition in WT, tPA–/–, and PAI–/– mice shows that 100% of WT mice displayed at least 1 aneurysm and that 64% were symptomatic. tPA–/– mice displayed less aneurysms formation (P=0.004) and rupture (P=0.017) with 60% of animals with no aneurysm. PAI–/– mice displayed a phenotype similar than WT animals. *P<0.05. **B**, Kaplan–Meier analyses of asymptomatic mice at 28 days postinduction showed a better rate of survival for tPA–/– mice and a worse rate of survival for PAI–/– mice when compared with WT animals. **C**, Magnetic resonance imaging assessment of the number of aneurysms on surviving animals at day 28 showed that the average number of aneurysms was significantly higher in WT and PAI–/– animals when compared with tPA–/– mice. *P<0.05. The final enrolled animal number was WT (n=11), tPA–/– (n=10), and PAI–/– (n=9).

and only 10% had ruptured aneurysms, 100% of the WT animals (n=11) displayed at least 1 aneurysm and 64% had ruptured aneurysms. Accordingly, Kaplan–Meier analyses of asymptomatic mice at 28 days postsurgery revealed a higher proportion of healthy animals in the tPA–/– group when compared with the WT group (respectively 90% and 36%; *P*=0.009; Figure 3B). PAI–/– mice displayed a pattern of unruptured and ruptured aneurysms similar to that of WT animals (*P*=0.22; Figure 3A). Indeed, in the PAI–/– group, 100% of animals (n=9) harbored at least 1 aneurysm and 89% had

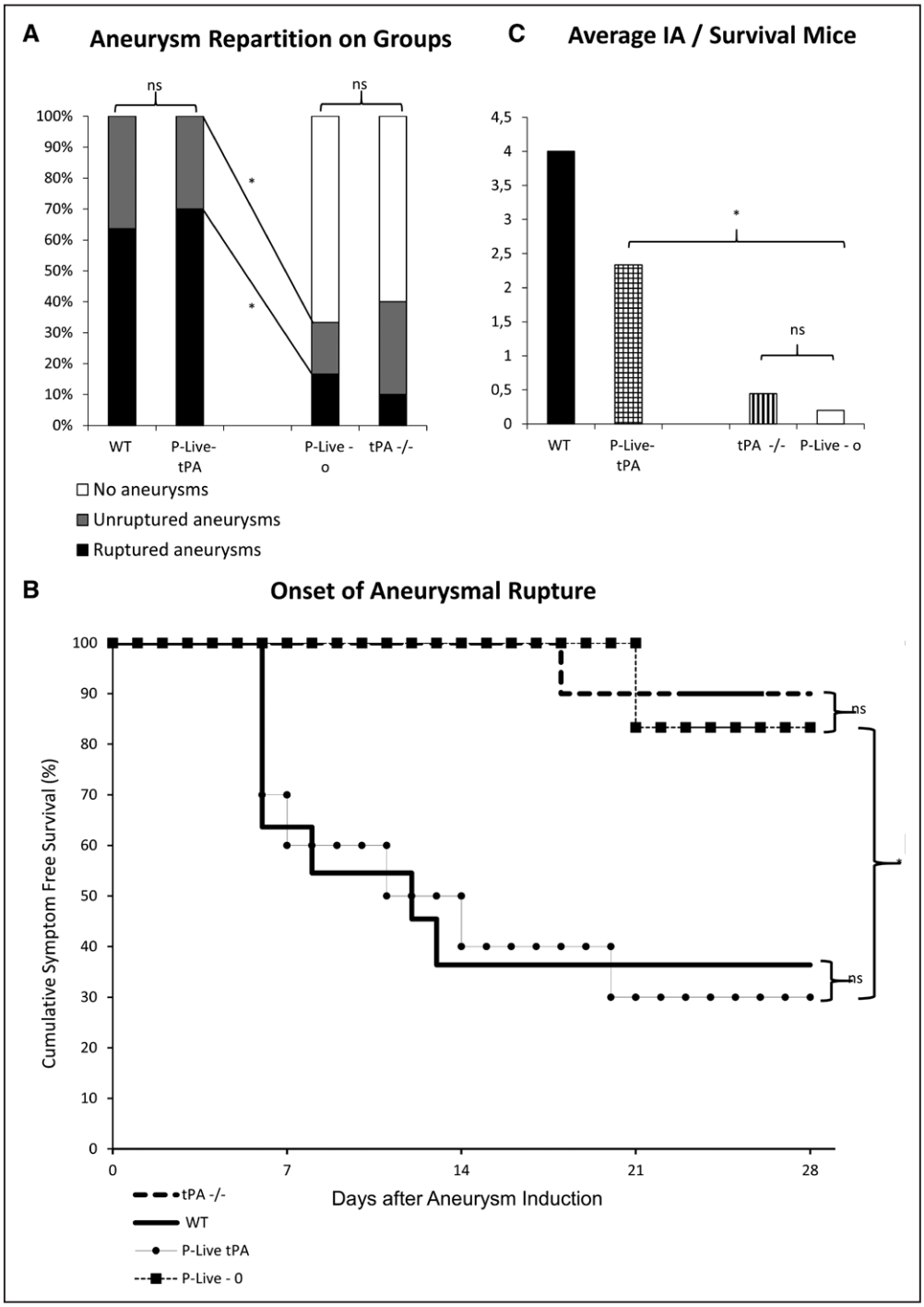

Figure 4. Vascular tPA (tissue-type plasminogen activator) contributes to aneurysms formation and rupture. Intracranial aneurysms (IAs) were induced in tPA deficient (tPA–/–) 2 days after the mice were transfected (hydrodynamic transfections as described in the Methods in the online-only Data Supplement) with a plasmid encoding for tPA (P-Live-tPA) or an empty vector (P-Live-o). **A**, 100% of P-Live-tPA animals presented at least 1 ruptured aneurysm compared with P-Live-o animals at day 28. **P*<0.05. **B**, Kaplan–Meier test revealed a better rate of survival for the P-Live-o mice when compared with P-Live-tPA animals. No significant difference was observed between wild-type (WT) and P-Live-tPA animals or between tPA–/– and P-Live-o animals. **C**, Number of aneurysms on surviving mice at 28 days showed that the average number of aneurysms was significantly higher in the P-Live-tPA animals than in the P-Live-o animals. **P*<0.05. The final enrolled animal number was P-Live-tPA group (n=10); P-Live-o group (n=6).

ruptured aneurysms. Nevertheless, the symptom-free survival Kaplan–Meier analysis revealed that PAI−/− mice displayed a significant higher rate of survival when compared with WT animals (P=0.049; Figure 3B). These results are explained by the fact that in PAI−/− mice, ruptures occurred earlier than in WT mice (Figure 3B). MRI analyses of the number of aneurysms in surviving mice at the end of the experiment at 28 days are shown in Figure 3C. WT (P=0.003) and PAI−/− (P=0.002) groups had more aneurysms than tPA−/− group.

Vascular tPA Contributes to IAs Formation and Subsequent Rupture

Thus, we sought to determine which tPA vascular or parenchymal, contributed to aneurysm formation and subsequent rupture in our model. Hydrodynamic transfections in tPA−/− mice with a pLIVE plasmid encoding for the rat tPA (P-Live-tPA) induced a vascular release of proteolytically active tPA in the circulation as soon as 24 hours after hepatic transfection,[23,24] compared with the levels of tPA present in the circulation of control empty P-Live plasmid (P-Live-o; Figure ID in the online-only Data Supplement). Although in the P-Live-tPA group (n=10), 100% of animals displayed at least 1 aneurysm at day 28 with 70% of them ruptured (Figure 4A), in the P-Live-o group (n=6) only 33% of mice presented at least 1 aneurysm, and only 17% were symptomatic (Figure 4A). Therefore, P-Live-tPA animals presented significantly more aneurysms (P=0.008) with an increased number of ruptured aneurysms (P=0.059) than P-Live-o animals. Accordingly, the symptom-free survival Kaplan–Meier analysis (Figure 4B) shows a better rate of survival for P-Live-o mice than for P-Live-tPA animals (P=0.028). Moreover, regarding surviving mice at the end of the experiment (Figure 4C), P-Live-tPA mice presented a higher average number of aneurysms (P=0.036) than P-Live-o mice. It is interesting to note (Figure 4A and 4B) that the symptom-free survival rate of P-Live-tPA was not different from that of WT mice (P=0.908) and that the symptom-free survival rate of P-Live-o animals was similar to that of tPA−/− mice (P=0.74). Immunostainings for tPA performed in tPA−/− mice (Figure IIIA in the online-only Data Supplement) clearly show the absence of tPA in the endothelium, in the media, and in the adventitia of normal arteries. Interestingly, tPA−/− mice develop IAs when the tPA is overexpressed and released in the vasculature after hydrodynamic transfection of liver cells.

Immunostainings raised against CD4 revealed the presence of inflammatory cells in the thickened wall of IAs, in mice (Figure IIIB in the online-only Data Supplement). Moreover, a clear positive and specific staining for CD11 b was also observed in the wall of IAs in mice (Figure IIIC in the online-only Data Supplement). It is interesting to note that the stain was observed as well within the wall of IA than fixed at the endothelium during the diapedesis

Discussion

Our data reveal that tPA present in the circulation is a putative pharmacological target to prevent IAs formation and, thus, their subsequent ruptures. To our knowledge, we provide the first preclinical demonstration of a role of tPA in the formation of aneurysms. We show the presence of tPA and its substrate, plasminogen, in the arterial walls of cerebral aneurysms in both rodents and humans. Our preclinical data then demonstrate that the absence of tPA reduces the incidence of aneurysms. Interestingly, this effect is merely counteracted by the rescue of active tPA in the circulation. Accordingly, PAI-1−/− mice (PAI-1 being the main inhibitor of tPA in the circulation[26]) are highly sensitive to aneurysms formation and subsequent ruptures. The presence of tPA within the aneurysmal wall contrast with its location site in the luminal part of the endothelial cells of normal arteries (Figure 2B and 2C; Figure IIIA in the online-only Data Supplement). tPA−/− mice develop IAs only when the tPA is overexpressed in the blood stream (Figure 4A and 4B). These data suggest that the tPA present in the blood stream is enough to promote aneurysms formation and rupture. Even if we did not properly investigate the source of the tPA present in the aneurysmal wall, our hypothesis that it comes from the blood stream is in agreement with the recent publications demonstrating the capacity of tPA to cross the blood–brain barrier.[13,14,24] Also, we can propose that the vascular tPA is responsible for aneurysms formation.

Although the involvement of tPA in aneurysms formation is similarly observed between either WT and tPA−/− mice or tPA−/− p-live-empty vector and tPA−/− Plive-tPA, differences in IAs rupture reached significance only between WT and tPA−/− mice. This could be explained by the fact that the expression of tPA is only transient after hydrodynamic transfection (from 1 to 7 days),[24] sufficient to induce aneurysms formation but may be too short to promote their rupture which can step afterward (38% from 7 to 14 days in our experiments, regardless of the genotype). This interesting shift suggests the continuity over time of the tPA influence on IAs because it has been reported in aortic aneurysms.[18] Because the size of IAs is mainly described as a key factor for IAs rupture,[2,5] we aimed to assess this parameter (data not shown). Probably because of important bias in the methodology, we did not evidence significant differences nor trend between groups on the size of IAs, which could have specified the mode of influence of tPA on the rupture of IAs.

Although aneurysmal formation and rupture may depend on several mechanisms,[2,5,7,9] our data demonstrate an important contribution of tPA. Different mechanisms could explain our finding because the MMPs can be activated by tPA either directly or indirectly through plasmin.[13,27] By their proteolytic activities, MMPs, especially MMP-2 and MMP-9, are also well known to contribute to the degradation of the internal elastic lamina, promoting IAs formation.[7,8,10,12] Similarly, it was reported that inflammation causes an overexpression and overactivation of MMPs, not compensated by the action of their inhibitors (tissue inhibitor of matrix metalloproteinases).[27,28] Moreover, tPA is known to upregulate the expression of MCP-1 (monocyte chemoattractant protein type 1), then to stimulate diapedesis and to participate in the infiltration process of macrophages within the arterial wall[29] as we experimentally found-it in our model (Figure IIIB and IIIC in the online-only Data Supplement). Thus, tPA could indirectly contribute to aneurysm formation and rupture through a proinflammatory path.[7,11,20] Our present data agree with this hypothesis, with the tPA present in the blood stream promoting the recruitment of macrophages in the IAs wall. These results are

in agreement with those reported from studies performed on aortic aneurysms that share some similarities with IAs.[16–18,28] Thus, some studies have suggested that the LRP-1 (low density lipoprotein related protein receptor 1) protected against elastin fiber fragmentation by reducing excess of protease activity in the artery wall.[28] These proteases include MMP-2 and -9, some of them being direct or indirect targets of tPA.[15,19,28] Even if abdominal aortic aneurysms and IAs present different clinical evolutions and responses to pharmacological therapies,[17,30] there are several similarities between the 2, and some pathophysiological cross pathways may be proposed, such as the role of tPA.

There are known direct inhibitors of tPA (such as neuroserpin and PAI-1) or indirect inhibitors (such as tranexamic acid via inhibition of plasmin) which could be used to prevent aneurysms formation and rupture.[13,14] Our data obtained from PAI–/– mice suggest that PAI-1 and PAI-1 mimetics[26] may be appropriate to prevent IAs formation and rupture. Additional studies are needed to address this important question. In conclusion, we propose the vascular tPA as a possible new target to prevent IA progression and rupture. However, because our present study was performed in a preclinical model of IAs, which does not completely fit with the pathogenesis of IAs formation and rupture in human, this conclusion should be cautioned. Further investigations are needed before translate these findings to clinic, thus, opening new avenues for the noninvasive prevention and treatment of IAs.

Acknowledgments

We thank Prof Carine Ali and Drs Anne-Laure Genevois and Gabriel Ichim for their help to edit this article.

Sources of Funding

This work was supported by grants from the French National Institute for Health and Medical Research and the Caen Normandie University, Fonds Européens de Développement Economique et Régional Normandie. This work is also part of an Agence Nationale de la Recherche program entitled PREDIC (prevent delayed ischemia), ANR16-CE19-004-01.

Disclosures

None.

References

1. Vlak MH, Algra A, Brandenburg R, Rinkel GJ. Prevalence of unruptured intracranial aneurysms, with emphasis on sex, age, comorbidity, country, and time period: a systematic review and meta-analysis. *Lancet Neurol*. 2011;10:626–636. doi: 10.1016/S1474-4422(11)70109-0.
2. Ishibashi T, Murayama Y, Urashima M, Saguchi T, Ebara M, Arakawa H, et al. Unruptured intracranial aneurysms: incidence of rupture and risk factors. *Stroke*. 2009;40:313–316. doi: 10.1161/STROKEAHA.108.521674.
3. Alleyne CH Jr. Aneurysmal subarachnoid hemorrhage: have outcomes really improved? *Neurology*. 2010;74:1486–1487. doi: 10.1212/WNL.0b013e3181e0ef1a.
4. Sandvei MS, Mathiesen EB, Vatten LJ, Müller TB, Lindekleiv H, Ingebrigtsen T, et al. Incidence and mortality of aneurysmal subarachnoid hemorrhage in two Norwegian cohorts, 1984-2007. *Neurology*. 2011;77:1833–1839. doi: 10.1212/WNL.0b013e3182377de3.
5. Bacigaluppi S, Piccinelli M, Antiga L, Veneziani A, Passerini T, Rampini P, et al. Factors affecting formation and rupture of intracranial saccular aneurysms. *Neurosurg Rev*. 2014;37:1–14. doi: 10.1007/s10143-013-0501-y.
6. Steiner T, Juvela S, Unterberg A, Jung C, Forsting M, Rinkel G; European Stroke Organization. European stroke organization guidelines for the management of intracranial aneurysms and subarachnoid haemorrhage. *Cerebrovasc Dis*. 2013;35:93–112. doi: 10.1159/000346087.
7. Chalouhi N, Ali MS, Jabbour PM, Tjoumakaris SI, Gonzalez LF, Rosenwasser RH, et al. Biology of intracranial aneurysms: role of inflammation. *J Cereb Blood Flow Metab*. 2012;32:1659–1676. doi: 10.1038/jcbfm.2012.84.
8. Frösen J, Piippo A, Paetau A, Kangasniemi M, Niemelä M, Hernesniemi J, et al. Remodeling of saccular cerebral artery aneurysm wall is associated with rupture: histological analysis of 24 unruptured and 42 ruptured cases. *Stroke*. 2004;35:2287–2293. doi: 10.1161/01.STR.0000140636.30204.da.
9. Penn DL, Witte SR, Komotar RJ, Sander Connolly E Jr. The role of vascular remodeling and inflammation in the pathogenesis of intracranial aneurysms. *J Clin Neurosci*. 2014;21:28–32. doi: 10.1016/j.jocn.2013.07.004.
10. Chu Y, Wilson K, Gu H, Wegman-Points L, Dooley SA, Pierce GL, et al. Myeloperoxidase is increased in human cerebral aneurysms and increases formation and rupture of cerebral aneurysms in mice. *Stroke*. 2015;46:1651–1656. doi: 10.1161/STROKEAHA.114.008589.
11. Hashimoto T, Meng H, Young WL. Intracranial aneurysms: links among inflammation, hemodynamics and vascular remodeling. *Neurol Res*. 2006;28:372–380. doi: 10.1179/016164106X14973.
12. Aoki T, Kataoka H, Morimoto M, Nozaki K, Hashimoto N. Macrophage-derived matrix metalloproteinase-2 and -9 promote the progression of cerebral aneurysms in rats. *Stroke*. 2007;38:162–169. doi: 10.1161/01.STR.0000252129.18605.c8.
13. Vivien D, Gauberti M, Montagne A, Defer G, Touzé E. Impact of tissue plasminogen activator on the neurovascular unit: from clinical data to experimental evidence. *J Cereb Blood Flow Metab*. 2011;31:2119–2134. doi: 10.1038/jcbfm.2011.127.
14. Macrez R, Ortega MC, Bardou I, Mehra A, Fournier A, Van der Pol SM, et al. Neuroendothelial NMDA receptors as therapeutic targets in experimental autoimmune encephalomyelitis. *Brain*. 2016;139(pt 9):2406–2419. doi: 10.1093/brain/aww172.
15. Kadoglou NP, Liapis CD. Matrix metalloproteinases: contribution to pathogenesis, diagnosis, surveillance and treatment of abdominal aortic aneurysms. *Curr Med Res Opin*. 2004;20:419–432. doi: 10.1185/030079904125003143.
16. Oszajca K, Wroński K, Janiszewska G, Bieńkiewicz M, Bartkowiak J, Szemraj J. The study of t-PA, u-PA and PAI-1 genes polymorphisms in patients with abdominal aortic aneurysm. *Mol Biol Rep*. 2014;41:2859–2864. doi: 10.1007/s11033-014-3141-6.
17. Davis FM, Rateri DL, Daugherty A. Abdominal aortic aneurysm: novel mechanisms and therapies. *Curr Opin Cardiol*. 2015;30:566–573. doi: 10.1097/HCO.0000000000000216.
18. Lindholt JS. Activators of plasminogen and the progression of small abdominal aortic aneurysms. *Ann NY Acad Sci*. 2006;1085:139–150. doi: 10.1196/annals.1383.023.
19. Lo EH, Wang X, Cuzner ML. Extracellular proteolysis in brain injury and inflammation: role for plasminogen activators and matrix metalloproteinases. *J Neurosci Res*. 2002;69:1–9. doi: 10.1002/jnr.10270.
20. Gur-Wahnon D, Mizrachi T, Maaravi-Pinto FY, Lourbopoulos A, Grigoriadis N, Higazi AA, et al. The plasminogen activator system: involvement in central nervous system inflammation and a potential site for therapeutic intervention. *J Neuroinflammation*. 2013;10:124. doi: 10.1186/1742-2094-10-124.
21. Tada Y, Kanematsu Y, Kanematsu M, Nuki Y, Liang EI, Wada K, et al. A mouse model of intracranial aneurysm: technical considerations. *Acta Neurochir Suppl*. 2011;111:31–35. doi: 10.1007/978-3-7091-0693-8_6.
22. Makino H, Hokamura K, Natsume T, Kimura T, Kamio Y, Magata Y, et al. Successful serial imaging of the mouse cerebral arteries using conventional 3-T magnetic resonance imaging. *J Cereb Blood Flow Metab*. 2015;35:1523–1527. doi: 10.1038/jcbfm.2015.78.
23. Ahlén G, Frelin L, Holmström F, Smetham G, Augustyn S, Sällberg M. A targeted controlled force injection of genetic material in vivo. *Mol Ther Methods Clin Dev*. 2016;5:16016. doi: 10.1038/mtm.2016.16.
24. Marcos-Contreras OA, Martinez de Lizarrondo S, Bardou I, Orset C, Pruvost M, Anfray A, et al. Hyperfibrinolysis increases blood-brain barrier permeability by a plasmin- and bradykinin-dependent mechanism. *Blood*. 2016;128:2423–2434. doi: 10.1182/blood-2016-03-705384.
25. Makino H, Tada Y, Wada K, Liang EI, Chang M, Mobashery S, et al. Pharmacological stabilization of intracranial aneurysms in

mice: a feasibility study. *Stroke*. 2012;43:2450–2456. doi: 10.1161/STROKEAHA.112.659821.
26. Gong L, Proulle V, Fang C, Hong Z, Lin Z, Liu M, et al. A specific plasminogen activator inhibitor-1 antagonist derived from inactivated urokinase. *J Cell Mol Med*. 2016;20:1851–1860. doi: 10.1111/jcmm.12875.
27. Kang LI, Isse K, Koral K, Bowen WC, Muratoglu S, Strickland DK, et al. Tissue-type plasminogen activator suppresses activated stellate cells through low-density lipoprotein receptor-related protein 1. *Lab Invest*. 2015;95:1117–1129. doi: 10.1038/labinvest.2015.94.
28. Strickland DK, Au DT, Cunfer P, Muratoglu SC. Low-density lipoprotein receptor-related protein-1: role in the regulation of vascular integrity. *Arterioscler Thromb Vasc Biol*. 2014;34:487–498. doi: 10.1161/ATVBAHA.113.301924.
29. Lansley SM, Cheah HM, Varano Della Vergiliana JF, Chakera A, Lee YC. Tissue plasminogen activator potently stimulates pleural effusion via a monocyte chemotactic protein-1-dependent mechanism. *Am J Respir Cell Mol Biol*. 2015;53:105–112. doi: 10.1165/rcmb.2014-0017OC.
30. Zhou X, Ji WJ, Tu Y, Yao M, Li YM. Abdominal aortic aneurysm and cerebral aneurysm present different pathological evolutions and responses to pharmacological therapy. *Med Hypotheses*. 2007;68:601–606. doi: 10.1016/j.mehy.2006.06.062.

Stroke
Journal of the American Heart Association

Vascular Tissue-Type Plasminogen Activator Promotes Intracranial Aneurysm Formation

Paul-Emile Labeyrie, Romain Goulay, Sara Martinez de Lizarrondo, Marie Hébert, Maxime Gauberti, Eric Maubert, Barbara Delaunay, Benjamin Gory, Francesco Signorelli, Francis Turjman, Emmanuel Touzé, Patrick Courthéoux, Denis Vivien and Cyrille Orset

Stroke. published online July 28, 2017;
Stroke is published by the American Heart Association, 7272 Greenville Avenue, Dallas, TX 75231

Print ISSN: 0039-2499. Online ISSN: 1524-4628

VASCULAR TISSUE-TYPE PLASMINOGEN ACTIVATOR (tPA) PROMOTES INTRACRANIAL ANEURYSM FORMATION

ONLINE SUPPLEMENT

SUPPLEMENTAL METHODS

Mice

Male mice (20-25g /2 months, CURB) were housed (2 to 3 mice per cage) on a 12h light/dark cycle, with *ad libitum* access to food and water. Three different mouse strains were used: tissue-type plasminogen activator knockout mice (tPA-/-, n=31), Plasminogen Activator Inhibitor-1 knockout mice (PAI-/-, n=12) and their wild type littermates (WT, n=12) all on a C57BL/6J background. Animals were randomly assigned to the different experimental groups.

Induction of intracranial aneurysms

IAs were induced as described by Hashimoto et al.[1,2]. Briefly, animals were deeply anesthetized using isoflurane 5% in a gas mixture of 70% NO_2/30% O_2 and maintained in 2% isoflurane (70% NO_2/30% O_2) during surgery. Mice were placed in a stereotaxic device and a craniotomy was performed using a cooled drill at the following coordinate from the Bregma - 2.5 posterior, +2.5 lateral and +5.5 deep. Using a thermoformed glass micropipette, 2.5 µL of elastase (35 mU diluted in saline solution; Sigma-Aldrich, L'isle d'Abeau, France) were injected over 10 minutes in the right basal cistern. The stereotaxic injection was immediately followed by subcutaneous implantation of an osmotic pump (p1001, Alzet®, Durect Corporation, Cupertino, USA) filled with angiotensin-II (800µg in 90µl saline solution, Sigma Aldrich, L'isle d'Abeau, France) allowing a diffusion rate of 37ng/ min over 14 days. An analgesic coverage was performed by subcutaneous injection of 100 µL of buprenorphine solution at 0.02mg/mL, 0.1 mg/kg body weight per animal (Buprenorphine Arrow, Laboratoire Arrow, Lyon, France). To ascertain the induction and check the profile of systemic hypertension induced by angiotensin II, repeated blood pressure measurements were blindly made within experimental groups. In all the three groups of mice (WT, tPA-/- and PAI-/-), systolic blood pressure measurement by the tail-cuff method was used in conscious mice as recommended in previous studies[2,3]. At day 2, a MRI was performed to exclude animals presenting a brain hemorrhage caused by the stereotaxic injection. Each animal was evaluated for inclusion criterion using a semi-quantitative Aneurysm Induction Invasiveness Score (AIIS) composed of 4 items (A: craniotomy, B: elastase injection, C: waking up, and D: MRI control) each quoted from 1 to 4 (Supplemental figure 1.A). All animals with a score over 7 were excluded from the study.

Neurological evaluation

All animals were analyzed twice a day for detection of neurological symptoms and weight loss over a period of 28 days post-induction. Weight loss was considered significant for a body weight loss of 10% or more per 24 hours. Neurological symptoms[2,3] were quantified as follows: inflexion of the torso and forelimbs on lifting of the whole animal by the tail; circling to one side with a normal posture at rest; leaning to one side at rest; no spontaneous activity. Symptomatic mice were immediately scanned by 7T MRI for the identification of intracranial hemorrhages and of ruptured aneurysms. The period before symptoms occurs, mice were considered as symptom free surviving animals and this time was evaluated and quoted per day after aneurysm induction. At 28 days marking the term of the study, all asymptomatic mice were scanned by 7T MRI prior to euthanasia as their MRI analyses were also used to estimate the number of unruptured aneurysms as well as the absence of bleeding. IAs lesion were

observed on each mouse, at the acute phase of rupture when symptomatic and at the end of the experiment (day 28) in the absence of rupture.

Magnetic Resonance Imaging analysis

Experiments were carried out on a Pharmascan 7T/12 cm system using surface coils (Bruker, Germany). During acquisitions, anesthesia was maintained using isoflurane 1.5% (70%/30% mixture of NO_2/O_2). T2*-weighted sequence (T2*W) were acquired using a FLASH (fast low angle shot) sequence and used to detect intracranial hemorrhage as a specific hyposignal [4]. 3D T1 Contrast Enhanced Weighted (3DT1-CE-W) sequence after intra peritoneal gadolinum injection (Gadovist® 1mg/kg, Guerbet, Villepinte, France) was performed to visualize IA defined as an abnormal sacciform outpouching of the wall of intracranial arteries of which the diameter is >150% of the parent artery diameter[4].

Two observers including a 5 year-experienced neuroradiologist specialist on aneurysm disease reviewed the images.

Hydrodynamic transfection of tPA

*Generation of pLIVE plasmid*s: the coding sequence for rat tPA was inserted into a mouse hepatocyte specific plasmid (pLIVE) (Supplemental Figure 1.B).

Hydrodynamic transfection: Hydrodynamic transfections were performed as previously described[5,6]. To assess the time course of efficiency of gene delivery, we have previously investigated [6] the presence of active and free (non-complexed) plasmatic tPA (and other possible plasminogen activators) by direct fibrin zymography following sodium dodecylsulphate polyacrylamide gel electrophoresis (SDS-PAGE), performed from plasma samples harvested before and after hepatic (hydrodynamic) transfection at day 1, 2, 3, 5, 7 and 14 [6]. Then, PA-/- mice considered for IA induction, were injected two days before induction with 100µg of pLIVE vector encoding for tPA (n=11) or empty pLIVE vector (n=9). A large volume, 10% of body weight, of plasmid-containing saline buffer was injected in the tail vein in less than 5 seconds (Supplemental Figure 1.C) [5]. Then, sentinel mice induced for IA were used to control levels of active plasmatic tPA, 24 hours after hydrodynamic transfection (Supplemental Figure 1.D) (time when the highest plasmatic levels of active tPA are reached), as previously described [6]. Human tPA (Actilyse®, Boehringer Ingelheim Paris, France) and plasmin (Enzyme Research Laboratoires, South Bend, USA) were used as loading controls [6].

Immunohistochemistry

Mouse tissue samples: each mouse was anesthetized and transcardially perfused with cold heparinized saline (50ml) followed by 100ml of fixative solution (PBS 0.1M: pH 7.4 containing 2% paraformaldehyde and 0.2% picric acid). Brains were cryoprotected (sucrose 20% in veronal buffer; 48h; 4°C) before freezing in Tissue-Tek (Miles Scientific, Naperfville, USA). Cryomicrotome-cut transversal sections (12 µm) were collected on poly-lysine slides and stored at -80%°C before processing.

Human samples: Human aneurysm samples were obtained during microsurgery by resecting the aneurysm sac distal to the clip closing the neck (F.S; Department of Vascular Neurosurgery, Hôpital Pierre Wertheimer; University of Lyon, France). Samples were obtained

from a 42-year-old woman, who suffered from SAH after a rupture of a 7mm large, middle cerebral artery IA. Tissues were immediately stored for two hours in fixative (PBS 0.1M: pH 7.4 containing 2% paraformaldehyde and 0.2% picric acid) then cryoprotected (sucrose 20% in veronal buffer; 48h; 4°C) before freezing in Tissue-Tek. Then, cryomicrotome-cut transversal sections (12µm) were collected on poly-lysine slides and stored at -80°C before processing.

Immunohistochemistry: Mouse and Human tissue sections were incubated overnight with the following primary antibodies as described in the corresponding legend, including a goat anti-collagen IV (1/1500, Southern Biotech, Birmingham, USA), a sheep anti-plasmin/plasminogen (Pln/Plg) polyclonal antibody (1/5000, kindly provided by HR Lijnen, University of Leuven, Belgium), a rabbit anti-tPA monoclonal (1/3000, provided by HR Lijnen, University of Leuven, Belgium), a rabbit anti-CD 11b monoclonal antibody (1/600, eBioscience, Paris, France) and a mouse anti-CD 4 monoclonal antibody (1/250, eBioscience, Paris, France) in veronal buffer (pH: 7.4). Primary antibodies were revealed with the appropriate secondary antibodies (FITC, Cy3 or Cy5, 1/500, Jackson Immunoresearch Suffolk, UK). Washed sections were cover slipped with antifade medium containing DAPI and images were digitally captured using a Leica DM6000 microscope-coupled coolsnap camera, analyzed with Metamorph® (Molecular Devices, Sunnyvale, USA) and Image J 1.46r (NIH, USA) softwares. For each animal, vascular wall and aneurysm were analyzed.

Statistical analysis

All results were expressed in the form of mean. Continuous variables were described as median and interquartile range (IQR), and compared using the nonparametric Kruskal Wallis test. Categorical variables were compared using Chi-2 or Fisher's exact test (unilateral test), as appropriate (SPSS 19, SPSS inc, Chicago USA). The survival analyses were performed by using Kaplan-Meier and log rank tests. The mice that did not show aneurysm formation were not excluded from the analysis. A p-value ≤ 0.05 was considered as significant.

SUPPLEMENTAL FIGURES AND FIGURE LEGENDS

Supplemental Figure I

A

Itemized Aneurysm Induction Invasiveness Score on mice

	I	II	III	IV
Craniotomy (= A)	no bleed	small bleeding yield spontaneously	small bleeding with local hemostasis needed	important bleeding extended local hemostasis
Technical success before awake (= B)	full technical success general anesthesia < 30 min	small technical failure general anesthesia < 40 min	serious technical failure	peri-operative death
Post operative clinical state (= C)	rapid awakening without altering the general condition	delayed awakening > 10 min without altering the general condition	delayed awakening > 20 min with alteration of the general condition < 60 min.	neurological deficit ; delayed awakening > 40 min; alteration of general condition > 2 hour.
MRI aspect at Day 2 on T2*W (= D)	no bleed	micro bleed micro needle path bleed	significant sub-arachnoid hemorrhage or localized bleeding without mass effect	intra-parenchymal bleeding with mass effect; massive sub-arachnoid bleeding
A + B + C + D =	4 ≤ AIIS CLINICAL SCORE ≤ 16			
All mice with any item > 3, all mice with AIIS Score > 7 are withdraw from the study				

B

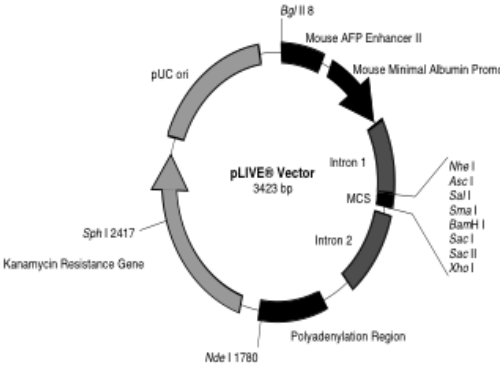

C

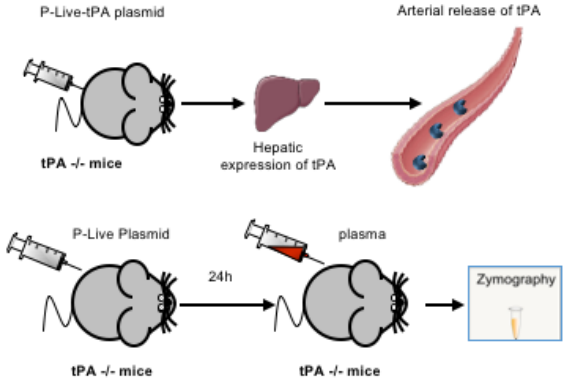

D

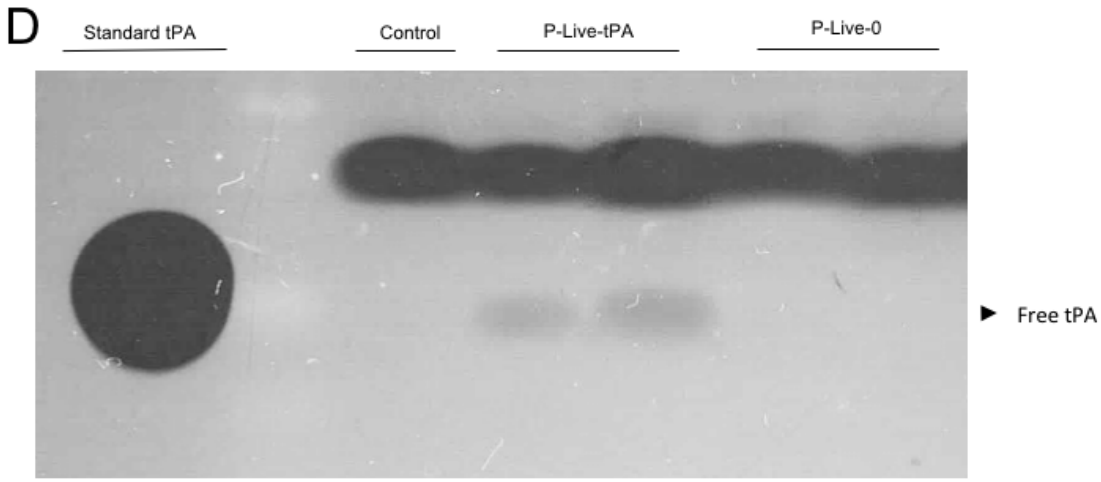

Supplemental Figure I. A) Detailed Aneurysm Induction Invasiveness Score **B)** Plasmid constructs used for hydrodynamic transfections with the cDNA encoding for tPA was placed under the control of a hepatocyte specific promoter. Two plasmids were generated, both with the same hepatocyte specific promoter: the first one is an empty plasmid (P-Live-o) and the second one containing a plasmid encoding for tPA (P-Live-tPA). **C)** Design of the procedure for hydrodynamic transfection. **D)** Fibrin-agar zymography assay performed in transfected mice (n =2 in P-Live-o group and n =2 in P-Live-tPA group) one day after hydrodynamic transfections revealed a strong expression and release of tPA in the blood stream in P-Live-tPA treated mice compared to control and P-Live-o mice.

Supplemental Figure II

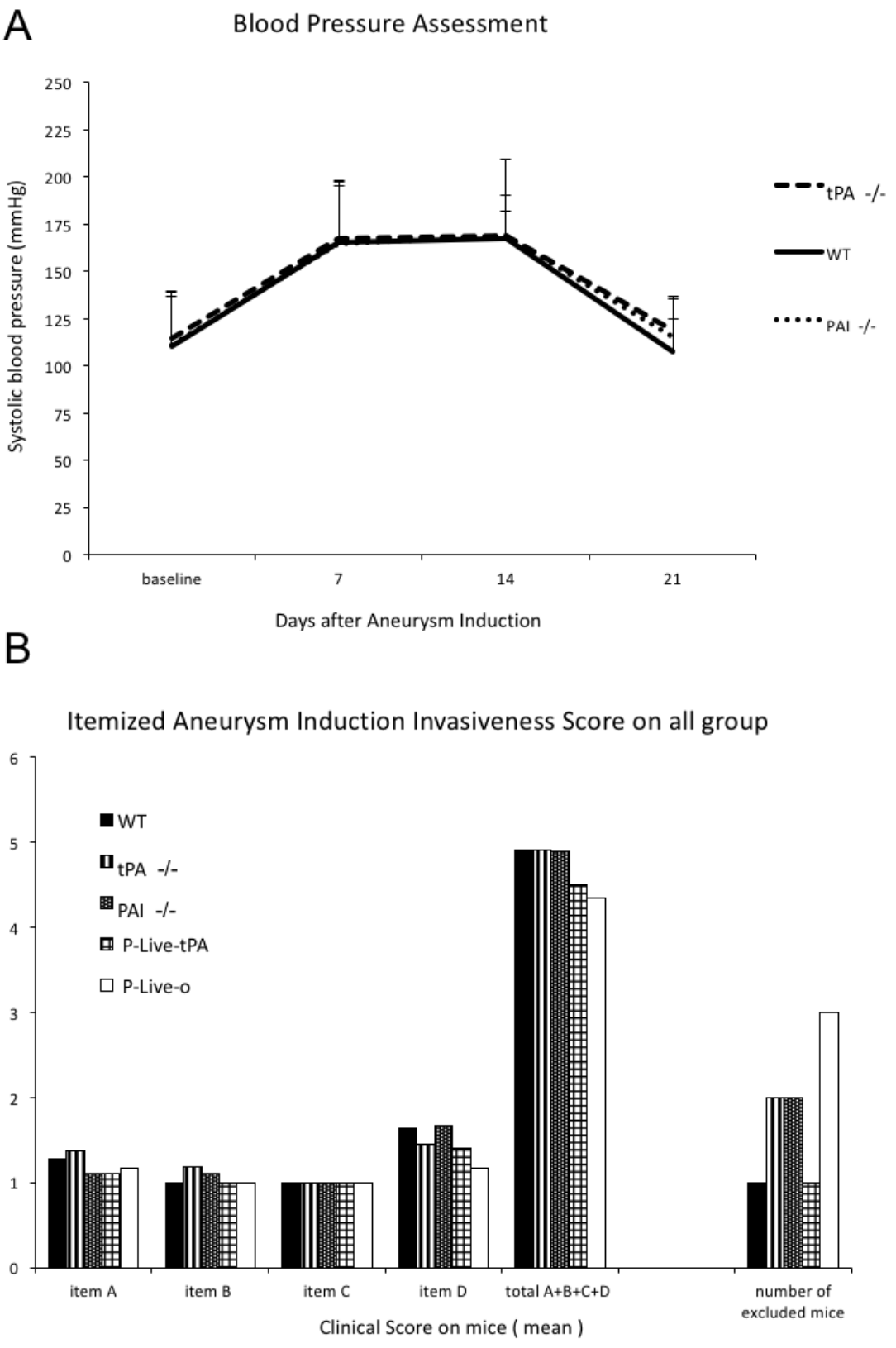

Supplemental Figure II. **A)** Assessment of the systolic blood pressure using the tail cuff method showed that Angiotensin II treatment led to a significant increase of the systemic blood pressure. No difference was observed between groups **B)** No difference was found between Aneurysm Induction Invasiveness Score on groups. Excluded mice for each group: for tPA -/- n= 2 (one died during aneurysm induction and one was excluded at Day 2 because of an Aneurysm Induction Invasiveness score > 7); for WT, n=1 (excluded at Day 2 because of an Aneurysm Induction Invasiveness score > 7); for PAI -/-, n= 2 (one mouse was excluded at Day 2 because of an Aneurysm Induction Invasiveness score > 7 and one mouse died at day one post induction before examination); for -P-Live-tPA, n=1 (one mouse was excluded at Day 3 after dying from complication of stereotaxic injection procedure); for P-Live-o, n=3 (one mouse was excluded at Day because of an Aneurysm Induction Invasiveness score > 7, and two animals died at day 3 and day 4 without any documented relation with aneurysmal ruptures).

Supplemental Figure III

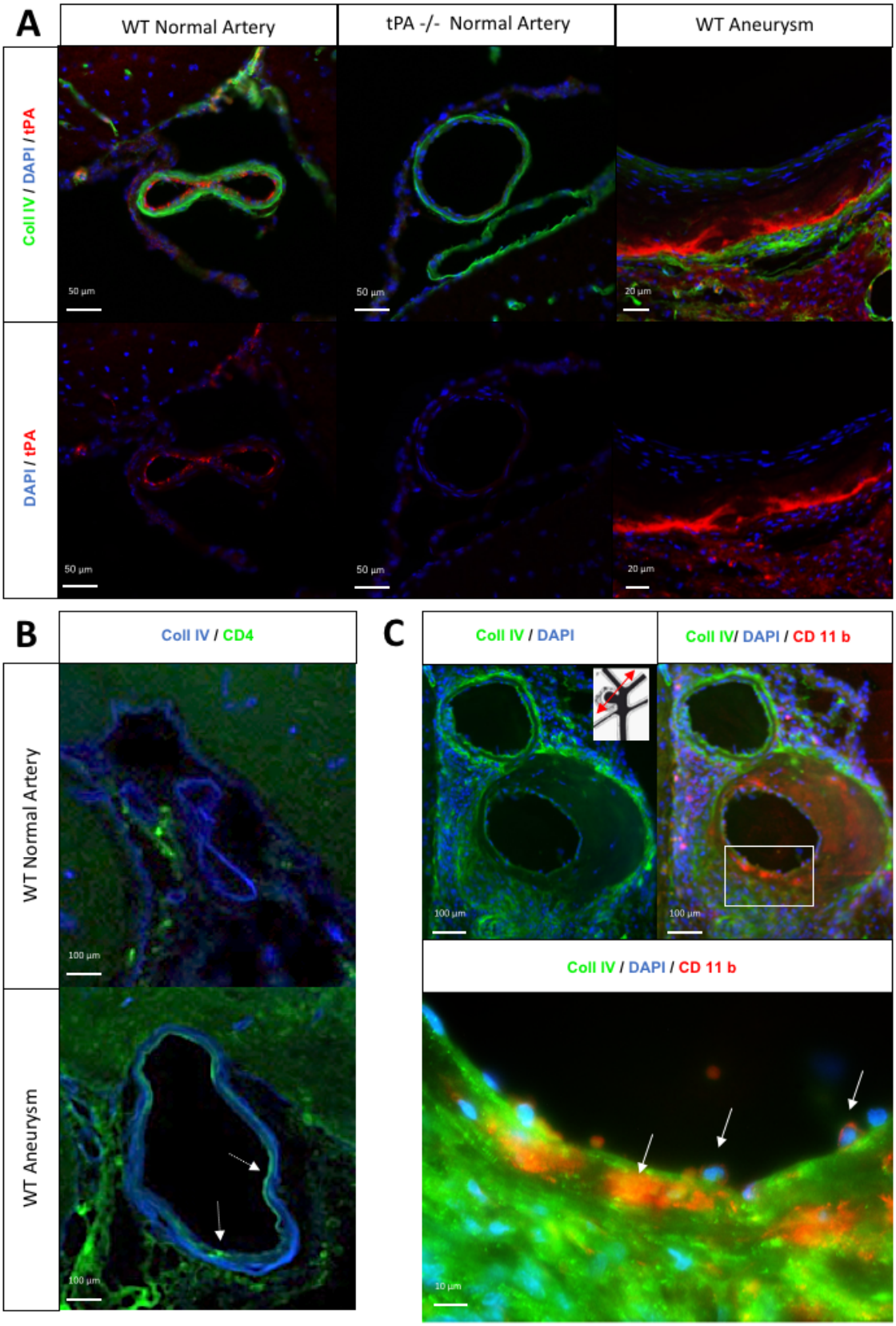

<u>Supplemental Figure III.</u> A) Representative immunohistochemistries performed from WT and tPA -/- mice, on normal (right) and aneurysmal artery (left) (collagen-IV in green, tPA in red and DAPI in blue. This result permit in WT mice to compare the repartition of tPA in normal artery as in aneurysm. And also to demonstrate the lack of tPA positive stain in the artery of tPA -/- mice. **B)** Representative immunohistochemistries exploring inflammatory process, performed from WT mice displaying unruptured intracranial aneurysms (collagen-IV in blue, tPA in red and CD 4 in green). Showing a specific stain of CD 4 (glycoprotein expressed on inflammatory celles) in the wall of the aneurysm on mice (white dotted arrow, lower panel) compared to his absence in the normal artery (upper panel). **C)** Immunohistochemistries exposing normal and aneurysmal artery on the same section (see section plan on left upper panel) of a WT mouse displaying ruptured intracranial aneurysms (collagen-IV in green, CD 11-b in red and DAPI in blue). This immunostaining highlighted a specific stain of the monocyte integrin implies in the diapedesis within the wall of the aneurysm as well as macrophage (white arrow, close-up on lower panel) during the diapedesis. This image show the inflammatory infiltration of the wall of IA induced in this model. Scale bars: A), 100 µm, 20µm; B), 100 µm; C) 100 µm, 10 µm.

SUPPLEMENTAL REFERENCES

1. Hashimoto T, Meng H, Young WL. Intracranial aneurysms: links among inflammation, hemodynamics and vascular remodeling. *Neurol. Res.* 2006;28:372–380.

2. Tada Y, Kanematsu Y, Kanematsu M, Nuki Y, Liang EI, Wada K, et al. A mouse model of intracranial aneurysm: technical considerations. *Acta Neurochirurgica Suppl*. 2011;111:31-35

3. Makino H, Tada Y, Wada K, Liang EI, Chang M, Mobashery S, et al. Pharmacological Stabilization of Intracranial Aneurysms in Mice. *Stroke*. 2012;43:2450–2456.

4. Makino H, Hokamura K, Natsume T, Kimura T, Kamio Y, Magata Y, et al. Successful Serial Imaging of the Mouse Cerebral Arteries Using Conventional 3-T Magnetic Resonance Imaging. *J. Cereb. Blood Flow Metab.* 2015;35:1523–1527.

5. Ahlén G, Frelin L, Höolmstrm F, Smetham G, Augustyn S, Sällberg M. A targeted controlled force injection of genetic material in vivo. *Mol. Ther. - Methods Clin. Dev.* 2016;3:16016.

6. Marcos-Contreras O, Martinez de Lizarrondo S, Bardou I, Orset C, Pruvost M, Anfray A. et al. Hyperfibrinolysis increases blood–brain barrier permeability by a plasmin- and bradykinin-dependent mechanism. Blood. 2016;128:2423–2434

Stroke Online Supplement

Table I. Checklist of Methodological and Reporting Aspects for Articles Submitted to *Stroke* Involving Preclinical Experimentation

Methodological and Reporting Aspects	Description of Procedures
Experimental groups and study timeline	☑ The experimental group(s) have been clearly defined in the article, including number of animals in each experimental arm of the study. ☑ An account of the control group is provided, and number of animals in the control group has been reported. If no controls were used, the rationale has been stated. ☑ An overall study timeline is provided.
Inclusion and exclusion criteria	☑ A priori inclusion and exclusion criteria for tested animals were defined and have been reported in the article.
Randomization	☑ Animals were randomly assigned to the experimental groups. If the work being submitted does not contain multiple experimental groups, or if random assignment was not used, adequate explanations have been provided. ☑ Type and methods of randomization have been described. ☑ Methods used for allocation concealment have been reported.
Blinding	☑ Blinding procedures have been described with regard to masking of group/treatment assignment from the experimenter. The rationale for nonblinding of the experimenter has been provided, if such was not feasible. ☑ Blinding procedures have been described with regard to masking of group assignment during outcome assessment.
Sample size and power calculations	☑ Formal sample size and power calculations were conducted based on a priori determined outcome(s) and treatment effect, and the data have been reported. A formal size assessment was not conducted and a rationale has been provided.
Data reporting and statistical methods	☑ Number of animals in each group: randomized, tested, lost to follow-up, or died have been reported. If the experimentation involves repeated measurements, the number of animals assessed at each time point is provided, for all experimental groups. ☑ Baseline data on assessed outcome(s) for all experimental groups have been reported. ☑ Details on important adverse events and death of animals during the course of experimentation have been provided, for all experimental arms. ☑ Statistical methods used have been reported. ☑ Numeric data on outcomes have been provided in text, or in a tabular format with the main article or as supplementary tables, in addition to the figures.
Experimental details, ethics, and funding statements	☑ Details on experimentation including stroke model, formulation and dosage of therapeutic agent, site and route of administration, use of anesthesia and analgesia, temperature control during experimentation, and postprocedural monitoring have been described. ☑ Different sex animals have been used. If not, the reason/justification is provided. ☑ Statements on approval by ethics boards and ethical conduct of studies have been provided. ☑ Statements on funding and conflicts of interests have been provided.